nature

LETTERS

Long-term potentiation depends on release of D-serine from astrocytes

Christian Henneberger[1], Thomas Papouin[2,3], Stéphane H. R. Oliet[2,3] & Dmitri A. Rusakov[1]

Long-term potentiation (LTP) of synaptic transmission provides an experimental model for studying mechanisms of memory[1]. The classical form of LTP relies on N-methyl-D-aspartate receptors (NMDARs), and it has been shown that astroglia can regulate their activation through Ca^{2+}-dependent release of the NMDAR co-agonist D-serine[2–4]. Release of D-serine from glia enables LTP in cultures[5] and explains a correlation between glial coverage of synapses and LTP in the supraoptic nucleus[4]. However, increases in Ca^{2+} concentration in astroglia can also release other signalling molecules, most prominently glutamate[6–8], ATP[9] and tumour necrosis factor-α[10,11], whereas neurons themselves can synthesize and supply D-serine[12,13]. Furthermore, loading an astrocyte with exogenous Ca^{2+} buffers does not suppress LTP in hippocampal area CA1 (refs 14–16), and the physiological relevance of experiments in cultures or strong exogenous stimuli applied to astrocytes has been questioned[17,18]. The involvement of glia in LTP induction therefore remains controversial. Here we show that clamping internal Ca^{2+} in individual CA1 astrocytes blocks LTP induction at nearby excitatory synapses by decreasing the occupancy of the NMDAR co-agonist sites. This LTP blockade can be reversed by exogenous D-serine or glycine, whereas depletion of D-serine or disruption of exocytosis in an individual astrocyte blocks local LTP. We therefore demonstrate that Ca^{2+}-dependent release of D-serine from an astrocyte controls NMDAR-dependent plasticity in many thousands of excitatory synapses nearby.

To investigate the role of astrocytes in NMDAR-dependent LTP, we focused on Schaffer collateral (SC)–CA1 pyramidal cell synapses, a classical subject of LTP studies. We patched passive astrocytes in the stratum radiatum and monitored SC-mediated field excitatory postsynaptic potentials (fEPSPs) in their immediate vicinity (Fig. 1a, b, and Supplementary Fig. 1). A standard high-frequency stimulation (HFS) protocol induced LTP, which was indistinguishable from that induced without patching an astrocyte (Fig. 1c and Methods). Because the intracellular solution routinely contained the high-affinity Ca^{2+} indicator Oregon Green bis-(o-aminophenoxy)ethane-N,N,N',N'-tetraacetic acid-1 (OGB-1; 0.2 mM), these observations were in accord with studies documenting robust LTP near an astrocyte loaded with 10 mM EGTA[14–16]. However, exogenous Ca^{2+} buffers, although they suppress rapid Ca^{2+} transients, are unlikely to affect equilibrated (resting) free Ca^{2+} controlled by active homeostatic mechanisms. To constrain free astrocytic Ca^{2+} more efficiently, we 'clamped' its concentration at 50–80 nM, by adding 0.45 mM EGTA and 0.14 mM Ca^{2+} to the intracellular solution (Methods)[19]. Indeed, Ca^{2+} clamp abolished HFS-induced increases in Ca^{2+} concentration, which could be detected in astrocytes containing OGB-1 and EGTA only (Supplementary Fig. 2). Furthermore, biophysical simulations suggested that Ca^{2+} clamp could restrict Ca^{2+} nanodomains more efficiently than buffers alone (Supplementary Fig. 3).
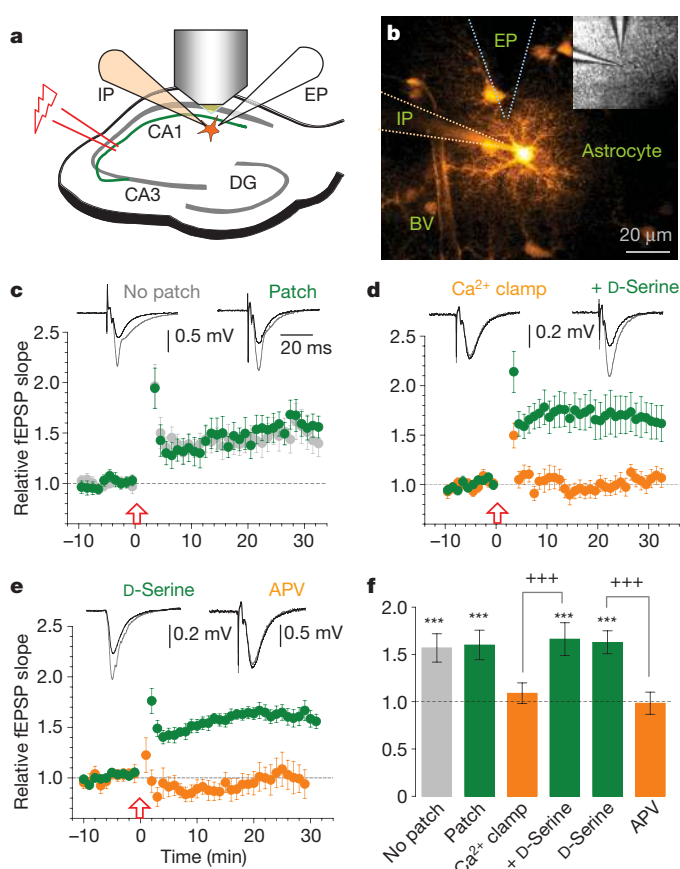

Figure 1 | Clamping astrocytic Ca^{2+} blocks LTP at nearby synapses in a D-serine-dependent manner. a, Experimental arrangement: IP, intracellular patch-pipette; EP, extracellular pipette; DG, dentate gyrus; green line, Schaffer collaterals. **b**, A typical patched astrocyte (Alexa Fluor 594, about 120 μm stack fusion). BV, blood vessel. Escape of Alexa to neighbouring cells can be seen. Inset: differential interference contrast at lower magnification. **c**, LTP of AMPAR fEPSPs in control conditions, with (green, n = 23) or without (grey, n = 28) astrocyte patched. Arrow indicates HFS onset; traces show characteristic AMPAR fEPSPs before (black) and after (grey) LTP induction; notations also apply in **c–e**. **d**, Clamping astrocytic Ca^{2+} (0.2 mM OGB-1, 0.45 mM EGTA, 0.14 mM $CaCl_2$) abolishes local LTP (orange, n = 19) whereas 10 μM D-serine rescues it (green, n = 10). **e**, LTP in 10 μM D-serine (green, 163 ± 12%, n = 8; no astrocyte patched) is no different from that in the control (**c**), suggesting saturation of either the NMDAR co-agonist site or the downstream induction mechanism. APV (50 μM) completely blocks LTP (orange, n = 12). **f**, Summary for experiments in **c–e**, as indicated. Results are presented as means ± s.e.m. for fEPSPs measured 25–30 min after HFS relative to baseline. Three asterisks, $P < 0.005$ (one-population t-test); three plus signs, $P < 0.002$ (two-population t-test).

[1]UCL Institute of Neurology, University College London, London WC1N 3BG, UK. [2]INSERM U862, Neurocentre Magendie, F-33077 Bordeaux, France. [3]Université de Bordeaux, F-33077 Bordeaux, France.

Strikingly, clamping the intra-astrocyte Ca^{2+} concentration completely suppressed LTP at nearby synapses, and the addition of 10 μM D-serine fully rescued it (Fig. 1d). D-Serine alone had no effect on LTP in control conditions (consistent with previous reports[20]), whereas the NMDAR antagonist (2R)-amino-5-phosphonovaleric acid (APV) completely blocked it (Fig. 1e, f). These observations imply that Ca^{2+}-dependent astrocyte activity could indeed control the supply of an NMDAR co-agonist essential for LTP induction[4,5,18,21]. To understand the underlying mechanisms, we recorded SC-evoked NMDAR fEPSPs near the patched astrocyte (Fig. 1a, b and Methods) while switching from a cell-attached to a whole-cell configuration (Fig. 2a). The control pipette solution (Methods) had little influence on NMDAR responses (change $10 \pm 7\%$ (mean ± s.e.m.) relative to baseline, $n = 6$; Fig. 2a, b), whereas Ca^{2+} clamp decreased them by $22 \pm 4\%$ ($n = 13$, $P < 0.0001$). This reduction was reversed by the subsequent application of D-serine ($10 \pm 9\%$ relative to baseline, $n = 7$, $P = 0.0012$; Fig. 2a, b and Supplementary Fig. 4), and the

presence of D-serine from the start blocked the inhibitory effect of Ca^{2+} clamp ($16 \pm 12\%$, $n = 7$; Fig. 2a, b). Ca^{2+}-dependent astrocyte signalling could therefore regulate the occupancy of the NMDAR co-agonist site.

In resting conditions, 10 μM D-serine increased NMDAR-mediated excitatory postsynaptic currents (EPSCs) in CA1 pyramidal cells (by $29 \pm 10\%$; $n = 5$, $P = 0.039$; Fig. 2c) as well as local NMDAR fEPSPs (by $25 \pm 3\%$, $n = 8$, $P < 0.001$; Supplementary Fig. 5), indicating that the NMDAR co-agonist sites were not saturated in baseline conditions, which is consistent with recent observations in hippocampal slices[22] and in vivo[23]. Interestingly, LTP induction had no long-term effect on the NMDAR co-agonist site occupancy: D-serine applied 25 min after induction brought about equal increases in NMDAR EPSCs (by $23 \pm 8\%$, $n = 6$, $P = 0.034$; Fig. 2c) and fEPSPs (by $25 \pm 9\%$; $n = 6$, $P = 0.042$; Supplementary Fig. 5), which were indistinguishable from the pre-induction effects. In contrast, even mild repetitive stimulation of SCs (ten stimuli at 50 Hz) was sufficient
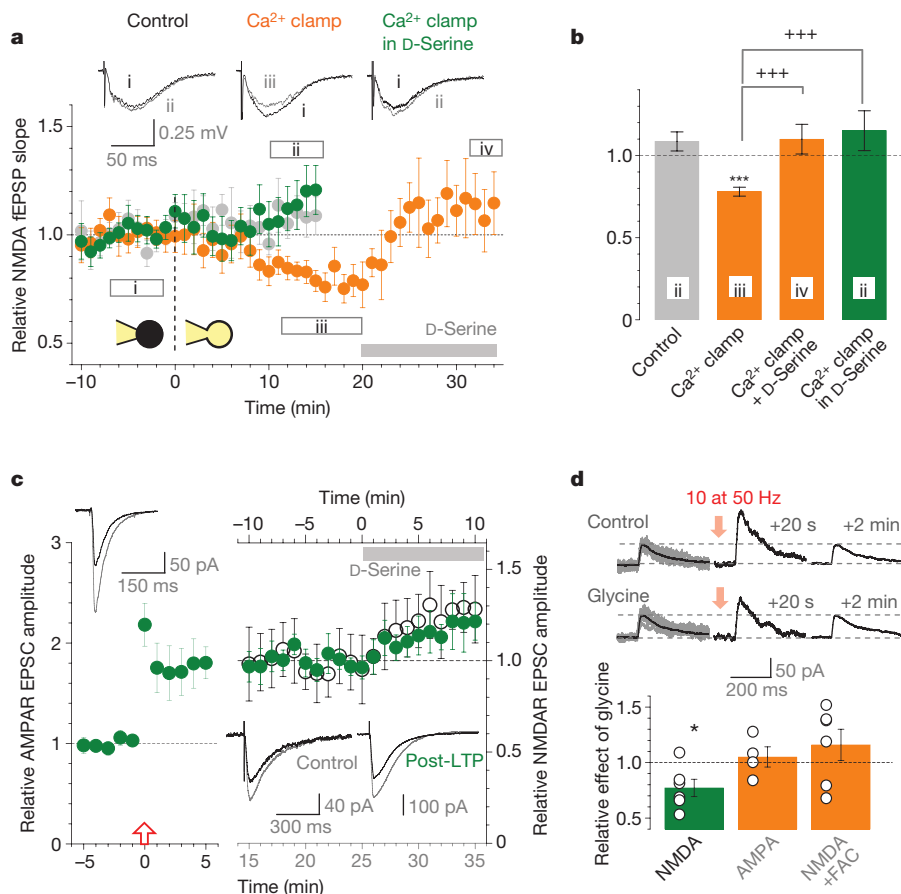

Figure 2 | Activation of the NMDAR co-agonist site is astrocyte-dependent and use-dependent. a, NMDAR fEPSP slope (Fig. 1a arrangement) monitored during the transition from cell-attached to whole-cell mode, as indicated. Grey circles, control ($n = 6$; Methods); orange, Ca^{2+} clamp ($n = 7$ throughout, $n = 13$ before D-serine application); green, Ca^{2+} clamp with 10 μM D-serine in bath ($n = 7$). Segments are averaging epochs; traces show examples (see also Supplementary Fig. 4). **b**, Summary of experiments shown in **a**. Results are presented as means ± s.e.m. (applies throughout); numerals indicate epochs in **a**. Three asterisks, $P < 0.0001$ (one-population t-test); three plus signs, $P < 0.005$ (two-population t-tests). **c**, Effect of D-serine on NMDAR EPSCs before and after LTP induction. Green circles, amplitude of AMPAR EPSCs ($n = 6$; left panel; $V_m = -70$ mV) and, subsequently, NMDAR EPSCs in the same cell after LTP (right panel; 10 μM 2,3-dihydroxy-6-nitro-7-sulphamoyl-benzo(f)quinoxaline (NBQX), $V_m = -10$ mV); grey segment, D-serine application. Open circles ($n = 5$; top axis, right panel), NMDAR EPSC amplitudes in no-LTP conditions. Traces: upper left, characteristic AMPAR EPSCs in control (black) and after LTP (grey); lower right, NMDAR EPSCs before (black) and after (grey)

application of D-serine, in control and after LTP, as indicated. **d**, A train of ten pulses at 50 Hz transiently potentiates synaptic NMDAR responses in a glycine-dependent and glia-dependent manner. Traces show examples of single-stimulus EPSCs including a prominent NMDAR-mediated component ($V_m = +40$ mV; no AMPAR blockade was used to ensure pharmacological continuity with LTP induction protocols) in baseline conditions (left; grey, individual traces; black, average), 20 s (middle) and 2 min (right) after the stimulus train, in control (upper row) and in 0.1 mM glycine (lower row). Bar graph: average ratio of after-train EPSC potentiation in glycine to after-train EPSC potentiation in control, for test experiments illustrated by traces (green; average change in the NMDAR-mediated response expressed as the area under the EPSC curve over the 100–300-ms after-peak interval: $-23 \pm 8\%$, $P = 0.032$, $n = 6$), and also for control experiments (orange) including AMPAR EPSCs (amplitude change $5 \pm 9\%$; $P = 0.41$, $n = 4$) and NMDAR EPSCs in FAC ($15 \pm 14\%$; $P = 0.32$, $n = 6$), as indicated (examples in Supplementary Fig. 6); circles, individual experiments.

to boost the co-agonist site occupancy transiently: short-term potentiation of the NMDAR-mediated EPSC component 20 s after the train was decreased by $20 \pm 7\%$ ($n = 6$, $P = 0.043$) when the co-agonist site was saturated by 0.1 mM glycine, before returning to the baseline level 2 min later (Fig. 2d). This was not due to changes in cell excitability or release probability because similar potentiation of α-amino-3-hydroxy-5-methyl-4-isoxazole propionic acid receptor (AMPAR) responses showed no sensitivity to glycine (Fig. 2d and Supplementary Fig. 6). Furthermore, the glial metabolic poison fluoroacetate (FAC, 5 mM) made the NMDAR EPSC potentiation also insensitive to glycine, thus implicating glia (Fig. 2d and Supplementary Fig. 6). In concord with these observations, HFS induced transient increases in Ca^{2+} concentration in 54% of astrocytes (consistent with earlier reports[24]) but no long-term changes in spontaneous Ca^{2+} activity (Supplementary Fig. 7).

If astrocytes enable LTP induction by increasing activation of the NMDAR co-agonist site, then decreasing the site availability should prevent LTP[25]. To replicate the roughly 25% decrease of NMDAR responses under astrocytic Ca^{2+} clamp (Fig. 2a, b), we used the selective NMDAR glycine-site blocker 5,7-dichlorokynurenic acid (DCKA) at 750 nM (Fig. 3a and Supplementary Fig. 8). Notably, 750 nM DCKA abolished LTP, similarly to 50 μM APV (Fig. 3a). Consistent both with these observations and with the Ca^{2+} clamp effects, FAC also decreased NMDAR fEPSPs by $23 \pm 4\%$ ($n = 16$, $P = 0.00017$; Supplementary Fig. 9a, b) and blocked LTP in a D-serine-sensitive manner (Fig. 3b, c). Although the mechanisms and specificity of FAC actions are incompletely understood, we confirmed that the effect of FAC on NMDAR fEPSPs paralleled that on LTP (Supplementary Fig. 9c, d), was absent in the presence of glycine,

and did not involve changes in release probability or axonal excitability (Supplementary Fig. 10).

However, such experiments provide no direct evidence for D-serine release from astroglia: an alternative possibility is that an NMDAR co-agonist is released from elsewhere, for example, neurons[12,13], in response to an unknown astrocytic signal. To investigate this, we blocked D-serine synthesis inside an astrocyte by using the relatively specific serine racemase inhibitor L-erythro-3-hydroxyaspartate (HOAsp)[26] loaded at 400 μM (to suppress competition from L-serine) but found no effect on local LTP (Fig. 3d). However, HOAsp does not influence D-serine itself and therefore cannot prevent release of the stored agonist. We therefore attempted to deplete the putative astrocytic pool of D-serine by applying HFS in the presence of APV. When APV was washed out and HFS was applied again, LTP induction was indeed suppressed, whereas the same protocol with no HOAsp loaded yielded robust potentiation (Fig. 3e, f). This result demonstrates causality between astrocytic synthesis of D-serine and local LTP.

How far do individual CA1 astrocytes extend their influence on LTP? Although astrocytes occupy separate domains[27], they can communicate through gap junctions[28], which were left intact in the present study. To determine whether these cells could act independently, we monitored LTP simultaneously in two neighbouring areas associated with two astrocytes. First, we confirmed that field potentials recorded through an astrocytic patch-pipette reliably represent local fEPSPs, with no bias from glutamate transporter or K^+ currents[14] (Supplementary Fig. 11). We next patched two neighbouring astrocytes and monitored SC-evoked 'astrocytic' fEPSPs (a-fEPSPs) representing the two respective areas (Fig. 4a–c). Clamping Ca^{2+} in one
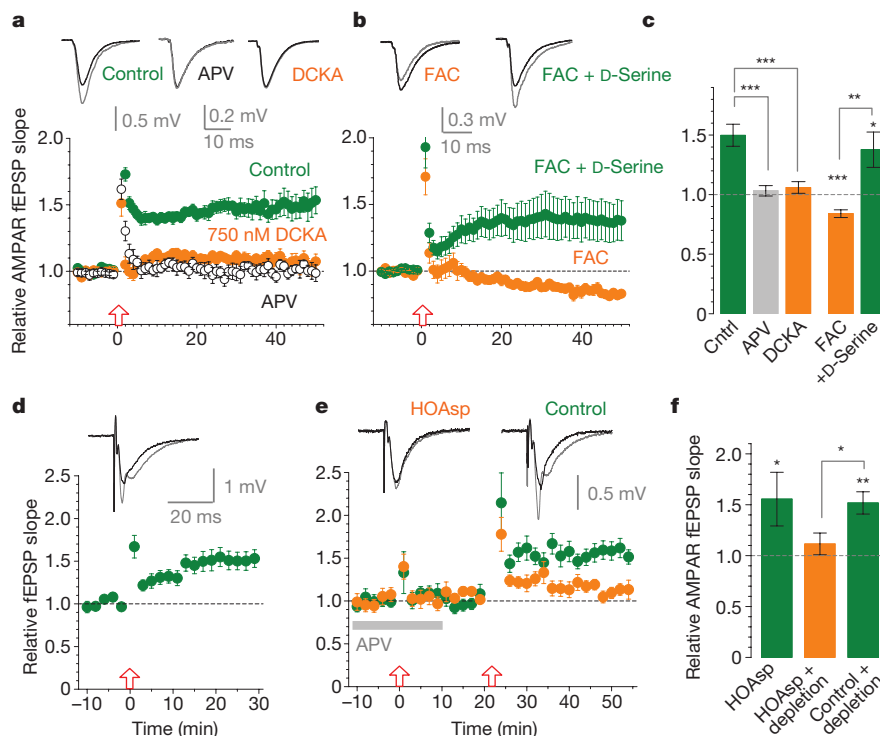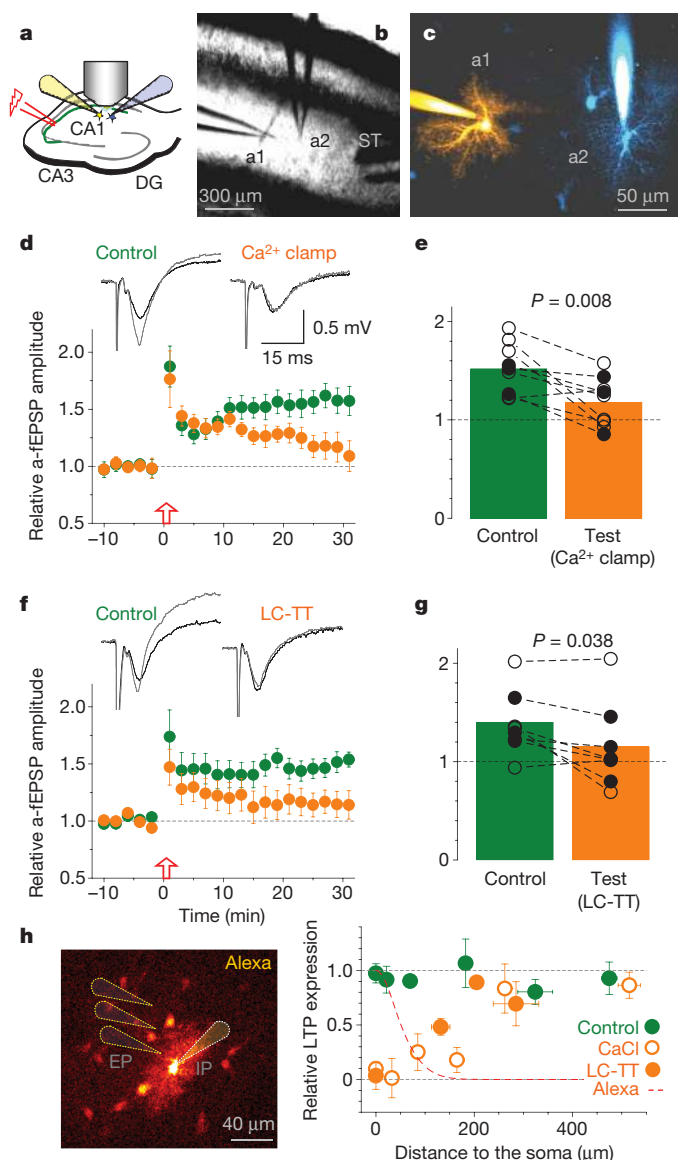

Figure 3 | LTP expression depends on the occupancy of the NMDAR co-agonist sites controlled by D-serine synthesis in a nearby astrocyte. a, LTP of AMPAR fEPSPs in control conditions ($n = 10$; green circles) is abolished by either 50 μM APV (open circles, $n = 12$) or 750 nM DCKA (orange; $n = 9$; dose–response curve in Supplementary Fig. 8). Traces show characteristic responses in control (black) and after LTP induction (grey). **b**, Incubation with 5 mM FAC for more than 50 min blocks LTP (orange circles, $n = 16$), whereas 10 μM D-serine rescues it (green circles, $n = 16$). Notation is as in **a. c**, Summary of experiments depicted in **a** and **b**. Results are presented as means $\pm$ s.e.m. (applies throughout). Asterisk, $P = 0.0127$; two asterisks, $P = 0.0014$; three asterisks, $P < 0.001$ (two-population t-test). **d**, Intra-

astrocyte HOAsp (400 μM) does not suppress LTP induction (potentiation is $50 \pm 15\%$, $n = 6$, $P = 0.021$; arrangement as in Fig. 1a); traces show average fEPSPs before (black) and after (grey) application of HFS, one-cell example; time scale applies to **d** and **e. e**, Intra-astrocyte HOAsp blocks induction of LTP (orange; fEPSP change $+12 \pm 11\%$, $n = 7$, $P = 0.32$) after depletion of D-serine with HFS in APV; arrows indicate HFS onset. Omitting HOAsp robustly induces LTP (green; $52 \pm 11\%$, $n = 6$, $P = 0.0052$). HOAsp was unlikely to affect glutamate metabolism because no rundown of glutamatergic responses was observed. **f**, Summary of experiments shown in **d** and **e**. Asterisk (left), $P = 0.021$; two asterisks, $P = 0.0052$ (one-population t-test); asterisk (right), $P = 0.024$ (two-population t-test).

Figure 4 | Individual astrocytes influence LTP induction mainly at nearby synapses. a, Experimental arrangement; notations as in Fig. 1a. **b, c**, An experiment seen in differential interference contrast (**b**) and in Alexa channel (**c**); a1 and a2, two patched astrocytes ($\lambda^{2P}_x = 800$ nm, ~150 μm z-stack; false colours: sequential staining of a1 and a2 followed by subtraction of a1 image from combined a1 + a2 image; Methods); st, stimulating electrode. **d**, Ca^{2+} clamp in test astrocyte suppresses local LTP, but not LTP near the neighbouring control astrocyte. Graph shows a-fEPSP amplitudes (means ± s.e.m.) recorded from the control (green) and test (orange) astrocytes ($n = 9$). Traces show respective characteristic a-fEPSPs (Supplementary Fig. 11) recorded before (black) and after (grey) LTP induction. Incomplete blockade of early potentiation near the test cell was probably due to delayed equilibration between the two dialysing pipettes. **e**, Summary of experiments in **d**; connected circles, recorded astrocyte pairs; black and hollow circles, experiments in which the test cell was, respectively, closer to and farther from the stimulating electrode (which might bias LTP expression); P values were determined with a paired t-test ($n = 9$). **f, g**, Experiments similar to those in **d** and **e**, but with the test astrocyte loaded with LC-TT ($n = 8$). Other notation is as in **d** and **e**. Slow equilibration of high-molecular-mass LC-TT might explain the incomplete block of early potentiation near the test cell. **h**, Left panel, experimental arrangement (as in Fig. 1a, b): dotted cones, depictions of the extracellular pipette (EP) and intracellular pipette (IP). Graph: circles, relative potentiation (means ± s.e.m.) of AMPAR fEPSPs at different distances from the patched soma in control (green, $n = 34$), Ca^{2+}-clamp (open orange, $n = 48$) and LC-TT (filled orange, $n = 15$) experiments. The dashed red line shows the average emission intensity profile of Alexa (whole-cell loaded at 40 μM) escaping to neighbouring cells ($n = 215$ astrocytes imaged in eight three-dimensional stacks; details in Supplementary Fig. 13).

an activated astrocyte. The importance of D-serine in LTP does not exclude the potential role of astrocytic glutamate release[6,8], and the precise mechanisms acting on the microscopic scale require further investigation. Individual astrocytes occupy about 9×10^4 μm^3 of CA1 neuropil (while overlapping by only 3–10%)[27], and the numeric synaptic density in this area is about 2 μm^{-3} (ref. 30), thus suggesting that a single astrocyte could affect synaptic input plasticity on hundreds of principal cells.

METHODS SUMMARY

Whole-cell recordings from passive astrocytes ($n = 146$) were made in stratum radiatum, area CA1 in acute transverse hippocampal slices prepared from adult rats. Cells (30–100 μm deep inside the slice) were loaded with a bright morphological tracer Alexa Fluor 594 and the high-affinity Ca^{2+} indicator OGB-1 and imaged in two-photon excitation mode ($\lambda^{2P}_x = 800$ nm). Field EPSPs were recorded with either an extracellular recording electrode placed in the immediate vicinity of the astrocyte soma under study or through the astrocytic patch pipette, as described. Whole-cell EPSCs were recorded from CA1 pyramidal cells. Electric stimuli were applied to Schaffer collateral fibres. LTP was induced by a standard HFS protocol (three 100-pulse trains at 100 Hz, 60 or 20 s apart). Inside the recorded astrocytes, conditions of Ca^{2+} homeostasis were altered by using intracellular solutions containing EGTA, OGB-1 and $CaCl_2$; the exocytosis machinery was suppressed with light-chain tetanus toxin; synthesis of D-serine was inhibited with the serine racemase inhibitor HOAsp.

1. Bliss, T. V. P. & Collingridge, G. L. A synaptic model of memory—long-term potentiation in the hippocampus. *Nature* **361**, 31–39 (1993).
2. Schell, M. J., Molliver, M. E. & Snyder, S. H. D-Serine, an endogenous synaptic modulator: localization to astrocytes and glutamate-stimulated release. *Proc. Natl Acad. Sci. USA* **92**, 3948–3952 (1995).
3. Mothet, J. P. et al. D-Serine is an endogenous ligand for the glycine site of the N-methyl-D-aspartate receptor. *Proc. Natl Acad. Sci. USA* **97**, 4926–4931 (2000).
4. Panatier, A. et al. Glia-derived D-serine controls NMDA receptor activity and synaptic memory. *Cell* **125**, 775–784 (2006).
5. Yang, Y. et al. Contribution of astrocytes to hippocampal long-term potentiation through release of D-serine. *Proc. Natl Acad. Sci. USA* **100**, 15194–15199 (2003).
6. Bezzi, P. et al. Prostaglandins stimulate calcium-dependent glutamate release in astrocytes. *Nature* **391**, 281–285 (1998).
7. Fellin, T. et al. Neuronal synchrony mediated by astrocytic glutamate through activation of extrasynaptic NMDA receptors. *Neuron* **43**, 729–743 (2004).

astrocyte suppressed LTP at nearby synapses but not at synapses near the neighbouring, control cell (Fig. 4d, e and Supplementary Fig. 12). A qualitatively identical result was obtained when putative vesicular exocytosis of D-serine[21,29] in the test astrocyte was suppressed by the light-chain tetanus toxin (LC-TT; Fig. 4f, g and Supplementary Fig. 12). In complementary experiments, we varied the distance between the extracellular recording pipette and the patched astrocyte. In Ca^{2+} clamp conditions, LTP partly recovered at 70–100 μm from the patched soma, reaching its full strength at approximately 200 μm, which is consistent with the profile of Alexa escaping to neighbouring cells (Fig. 4h and Supplementary Fig. 13). With a LC-TT-loaded astrocyte, LTP recovery occurred at markedly shorter distances (Fig. 4h), which is consistent with the toxin's inability to cross gap junctions.

Our findings demonstrate that induction of NMDAR-dependent LTP at excitatory hippocampal synapses depends on the availability of NMDARs provided by the Ca^{2+}-dependent release of D-serine from a local astrocyte. Repetitive synaptic activity transiently enhances D-serine supply by glia, paralleled by a short-term increase in astrocytic free Ca^{2+} concentration. Neighbouring astrocytes may have distinct effects on local synapses, but they also extend their influence beyond their morphological boundaries. This could potentially give rise to a Hebbian mechanism regulating hetero-synaptic NMDAR-dependent plasticity across a neuropil domain affected by

8. Perea, G. & Araque, A. Astrocytes potentiate transmitter release at single hippocampal synapses. *Science* **317**, 1083–1086 (2007).
9. Pascual, O. *et al.* Astrocytic purinergic signaling coordinates synaptic networks. *Science* **310**, 113–116 (2005).
10. Bezzi, P. *et al.* CXCR4-activated astrocyte glutamate release via TNFα: amplification by microglia triggers neurotoxicity. *Nature Neurosci.* **4**, 702–710 (2001).
11. Stellwagen, D. & Malenka, R. C. Synaptic scaling mediated by glial TNF-α. *Nature* **440**, 1054–1059 (2006).
12. Kartvelishvily, E., Shleper, M., Balan, L., Dumin, E. & Wolosker, H. Neuron-derived D-serine release provides a novel means to activate *N*-methyl-D-aspartate receptors. *J. Biol. Chem.* **281**, 14151–14162 (2006).
13. Miya, K. *et al.* Serine racemase is predominantly localized in neurons in mouse brain. *J. Comp. Neurol.* **510**, 641–654 (2008).
14. Diamond, J. S., Bergles, D. E. & Jahr, C. E. Glutamate release monitored with astrocyte transporter currents during LTP. *Neuron* **21**, 425–433 (1998).
15. Luscher, C., Malenka, R. C. & Nicoll, R. A. Monitoring glutamate release during LTP with glial transporter currents. *Neuron* **21**, 435–441 (1998).
16. Ge, W. P. & Duan, S. M. Persistent enhancement of neuron–glia signaling mediated by increased extracellular K$^+$ accompanying long-term synaptic potentiation. *J. Neurophysiol.* **97**, 2564–2569 (2007).
17. Fiacco, T. A. *et al.* Selective stimulation of astrocyte calcium *in situ* does not affect neuronal excitatory synaptic activity. *Neuron* **54**, 611–626 (2007).
18. Agulhon, C. *et al.* What is the role of astrocyte calcium in neurophysiology? *Neuron* **59**, 932–946 (2008).
19. Baker, P. F., Knight, D. E. & Umbach, J. A. Calcium clamp of the intracellular environment. *Cell Calcium* **6**, 5–14 (1985).
20. Duffy, S., Labrie, V. & Roder, J. C. D-Serine augments NMDA-NR2B receptor-dependent hippocampal long-term depression and spatial reversal learning. *Neuropsychopharmacology* **33**, 1004–1018 (2008).
21. Mothet, J. P. *et al.* Glutamate receptor activation triggers a calcium-dependent and SNARE protein-dependent release of the gliotransmitter D-serine. *Proc. Natl Acad. Sci. USA* **102**, 5606–5611 (2005).
22. Li, Y., Krupa, B., Kang, J. S., Bolshakov, V. Y. & Liu, G. S. Glycine site of NMDA receptor serves as a spatiotemporal detector of synaptic activity patterns. *J. Neurophysiol.* **102**, 578–589 (2009).
23. Fellin, T. *et al.* Endogenous nonneuronal modulators of synaptic transmission control cortical slow oscillations *in vivo*. *Proc. Natl Acad. Sci. USA* **106**, 15037–15042 (2009).
24. Porter, J. T. & McCarthy, K. D. Hippocampal astrocytes in situ respond to glutamate released from synaptic terminals. *J. Neurosci.* **16**, 5073–5081 (1996).
25. Cummings, J. A., Mulkey, R. M., Nicoll, R. A. & Malenka, R. C. Ca^{2+} signaling requirements for long-term depression in the hippocampus. *Neuron* **16**, 825–833 (1996).
26. Strisovsky, K., Jiraskova, J., Mikulova, A., Rulisek, L. & Konvalinka, J. Dual substrate and reaction specificity in mouse serine racemase: Identification of high-affinity dicarboxylate substrate and inhibitors and analysis of the β-eliminase activity. *Biochemistry* **44**, 13091–13100 (2005).
27. Bushong, E. A., Martone, M. E., Jones, Y. Z. & Ellisman, M. H. Protoplasmic astrocytes in CA1 stratum radiatum occupy separate anatomical domains. *J. Neurosci.* **22**, 183–192 (2002).
28. Rouach, N., Koulakoff, A., Abudara, V., Willecke, K. & Giaume, C. Astroglial metabolic networks sustain hippocampal synaptic transmission. *Science* **322**, 1551–1555 (2008).
29. Martineau, M., Galli, T., Baux, G. & Mothet, J. P. Confocal imaging and tracking of the exocytotic routes for D-serine-mediated gliotransmission. *Glia* **56**, 1271–1284 (2008).
30. Rusakov, D. A. & Kullmann, D. M. Extrasynaptic glutamate diffusion in the hippocampus: ultrastructural constraints, uptake, and receptor activation. *J. Neurosci.* **18**, 3158–3170 (1998).

METHODS

Preparation. Acute hippocampal slices 350 μm thick were obtained from 4–8-week-old male Sprague–Dawley or Wistar rats, in full compliance with national guidelines on animal experimentation. Slices were prepared in an ice-cold slicing solution containing (in mM): NaCl 75, sucrose 80, KCl 2.5, MgCl$_2$ 7, NaH$_2$PO$_4$ 1.25, CaCl$_2$ 0.5, and glucose 6 (osmolarity 300–310 mOsM), stored in the slicing solution at 34 °C for 15 min before being transferred to an interface chamber for storage in an extracellular solution containing (in mM) NaCl 119, KCl 2.5, MgSO$_4$ 1.3, NaH$_2$PO$_4$ 1, NaHCO$_3$ 26, CaCl$_2$ 2, glucose 10 (osmolarity adjusted to 295–305 mOsM with glucose). All solutions were continuously bubbled with 95% O$_2$/5% CO$_2$. Slices were allowed to rest for at least 60 min before recordings started. For recordings, slices were transferred to the submersion-type recording chamber and superperfused, at 23–26 °C, with artificial cerebrospinal fluid saturated with 95%O$_2$/5%CO$_2$ containing (in mM): NaCl 125, KCl 2.5, NaH$_2$PO$_4$ 1.25, NaHCO$_3$ 26, glucose 12 (pH 7.4; osmolarity 295–305 mOsM) in the presence of 1.3 mM Mg^{2+} and either 2.0 or 2.5 mM Ca^{2+} (where necessary, 50 μM picrotoxin was added to block GABA$_A$ receptors and a cut between CA3 and CA1 was made to suppress epileptiform activity).

Electrophysiology. Whole-cell recordings in astrocytes were obtained with standard patch pipettes (3–4 MΩ) filled with a 'control' intracellular solution containing (in mM) KCH$_3$O$_3$S 135, HEPES 10, disodium phosphocreatine 10, MgCl$_2$ 4, Na$_2$ATP 4, NaGTP 0.4 (pH adjusted to 7.2 with KOH, osmolarity 290–295 mOsM). Cell-impermeable dyes OGB-1 (200 μM; Invitrogen) and Alexa Fluor 594 hydrazide (40 μM; Invitrogen) were routinely added to the intracellular solution, unless indicated otherwise. Passive (protoplasmic) astrocytes were identified, in accordance with established criteria[14,31,32], by their small soma size (about 10 μm; detected in the Alexa emission channel), low resting potential (−86.8 ± 1.2 mV (mean ± s.e.m.), $n = 146$, no correction for the liquid-junction potential) and low input resistance (8.4 ± 0.6 MΩ, $n = 146$); we confirmed that they had passive (ohmic) properties and characteristic morphology of the arbour (Fig. 1 and Supplementary Fig. 1). Cells that showed atypical morphologies (3 out of 186) were discarded. Astrocytes were either held in voltage-clamp mode at their resting membrane potential or in current clamp. In some experiments recombinant LC-TT (1 μM; Quadratech Diagnostics Ltd) was included in the intracellular solution to disrupt vesicular release[33]. Where specified, 0.45 mM EGTA and 0.14 mM CaCl$_2$ were added to the control intracellular solution to clamp intracellular free Ca^{2+} at a steady-state concentration of 50–80 nM (calculation by WebMaxChelator). When required, the currently most effective specific serine racemase inhibitor HOAsp (Wako Chemicals; $K_i = 49$ μM)[26] was added to the intracellular solution.

Where indicated, the extracellular recording pipette was placed within the arbour or in the immediate vicinity of the patched astrocyte detected in the Alexa channel, less than 90 μm from the soma (Fig. 1). Synaptic responses were evoked by orthodromic stimulation (100 μs, 40–120 μA) of Schaffer collaterals by using either a bipolar or coaxial stimulation electrode placed in the stratum radiatum more than 200 μm from the recording electrodes. Field EPSPs (fEPSPs) were recorded with a standard patch pipette filled with the extracellular solution. Predominantly AMPAR-mediated fEPSPs (with no NMDAR blockers added) are denoted as AMPAR fEPSPs throughout the text; where required, NMDAR fEPSPs were isolated with 10 μM 2,3-dihydroxy-6-nitro-7-sulphamoyl-benzo(f)quinoxaline (NBQX) and 0.2 mM Mg^{2+} in the bath medium (except for post-LTP recordings performed in 1.3 mM Mg^{2+}, to maintain unchanged cell excitability).

The paired-pulse interval was 100 to 200 ms and the paired-pulse ratio was defined as the ratio of slope 2 to slope 1. In some experiments excitatory synaptic responses were monitored as field potentials recorded through one or two astrocyte patch-pipettes in current clamp mode (a-fEPSP; Supplementary Fig. 11). The stimulus intensity was normally set at about 70% of that triggering population spikes; stimuli were applied every 30 s for at least 15 min before the LTP was induced with three trains of HFS (100 pulses at 100 Hz), either 60 or 20 s apart. The slope of fEPSPs was subsequently monitored for 30–50 min.

Whole-cell recordings in CA1 pyramidal neurons were performed with an intracellular solution containing (in mM): potassium gluconate 130, KCl 5, HEPES, 10, disodium phosphocreatine 10, MgCl$_2$ 2, Na$_2$ATP 4, NaGTP 0.4, or, alternatively, caesium methane sulphonate 150, MgCl$_2$ 1.3, EGTA 1, HEPES 10, CaCl 0.1. AMPAR EPSCs in CA1 pyramidal cells were recorded at $V_m = -70$ mV, and NMDAR EPSCs were recorded in at $V_m = -10$ mV in the presence of 10 μM NBQX, unless indicated otherwise.

Where required, slices were preincubated in the glial metabolism inhibitor FAC[34] for at least 50 min, unless indicated otherwise; D-serine was added 10–15 min before LTP induction. Recordings were performed with a Multiclamp 700A or 700B (Molecular Devices). Signals were filtered at 3–6 kHz, digitized and sampled through an analogue-to-digital converter (National Instruments) at 10 kHz, and stored for offline analysis with either LabView (National Instruments) routines or pClamp9 software (Molecular Devices). Receptor blockers were purchased from Tocris, and FAC was purchased from Sigma-Aldrich.

Two-photon excitation imaging. We used a Radiance 2100 imaging system (Zeiss–Bio-Rad) optically linked to a femtosecond pulse laser MaiTai (SpectraPhysics-Newport) and integrated with patch-clamp electrophysiology[35]. Once in whole-cell mode, Alexa normally equilibrated across the astrocyte tree within 10–15 min. Astrocytes loaded with fluorescence indicators (see above) were imaged as three-dimensional stacks of 60–100 optical sections in the Alexa emission channel (540LP/700SP filter; $\lambda^{2P}_x = 800$ nm), collected in image frame mode (512 pixels × 512 pixels, eight-bit) at 0.5–1 μm steps.

For illustration purposes, the stacks were z-axis averaged with ImageJ routines (Rasband WS, ImageJ; National Institutes of Health; http://rsb.info.nih.gov/ij/ (1997–2008)). Transient Ca^{2+} signals evoked in patched astrocytes by HFS (Supplementary Fig. 2) were imaged in the OGB-1 (green) channel (515/30 filter) in line-scan mode (500 Hz), and corrected for focus fluctuations in the Alexa (red) channel, as detailed elsewhere[35–37] and illustrated in Supplementary Fig. 2.

To image Ca^{2+} activity simultaneously in a population of astrocytes (Supplementary Fig. 7), slices were incubated with the glia-specific dye sulforhodamine 101 (SR101, 5 μM; Invitrogen) and the Ca^{2+} indicator Fluo-4 acetoxymethyl ester or OGB-1 acetoxymethyl ester (5 μM; Invitrogen) in the presence of 0.04% Pluronic (Invitrogen), for 40–50 min at 37 °C and allowed to rest for at least 20 min. The viability of loaded slices was verified by monitoring fEPSPs in response to Schaffer collateral stimulation, as described earlier. Time-lapse imaging was performed by acquiring 800–20,000 pairs of SR101 and Fluo4/OGB-1 fluorescence image frames at a rate of 2 Hz (256 pixels × 256 pixels) or 7 Hz (64 pixels × 64 pixels). To evoke a Ca^{2+} response, HFS (100 pulses at 100 Hz) was delivered halfway through the experiment. In these experiments, time-dependent fluorescent transients were expressed as F/F_0 where F denotes the averaged, background-corrected Fluo-4/OGB-1 fluorescence of a SR101 positive (astrocytic) soma.

Visualization of astrocytic pairs and separating images of individual astrocytes in dual-patch experiments (Fig. 4) was performed with the following routine: first, cell 1 was patched, the dye was allowed to equilibrate and the resulting 'cell 1 image' (three-dimensional stack) was stored; second, cell 2 was patched, the dye was equilibrated and the resulting 'cell 1 + cell 2 image' was stored; third, 'cell 1 image' was subtracted from 'cell 1 + cell 2 image', yielding the fluorescent 'cell 2 image'. Comparing 'cell 1 image' and 'cell 2 image' could be used to reveal staining (diffusion) overlap between the two cells, which could be revealed with false-colour tables applied to the two images. Image analyses were performed offline with ImageJ.

Statistics. Group data are routinely reported as means ± s.e.m. indicated otherwise, and the statistical difference between the population averages was estimated with the t-test (for paired or independent samples). Two-tailed tests were routinely used, and sample pairing was used where appropriate, for example when monitoring real-time changes in a parameter against its baseline value or when comparing cells in paired recordings.

31. Bergles, D. E. & Jahr, C. E. Glial contribution to glutamate uptake at Schaffer collateral-commissural synapses in the hippocampus. *J. Neurosci.* **18**, 7709–7716 (1998).
32. Volterra, A. & Meldolesi, J. Astrocytes, from brain glue to communication elements: the revolution continues. *Nature Rev. Neurosci.* **6**, 626–640 (2005).
33. Xu, T., Binz, T., Niemann, H. & Neher, E. Multiple kinetic components of exocytosis distinguished by neurotoxin sensitivity. *Nature Neurosci.* **1**, 192–200 (1998).
34. Szerb, J. C. & Issekutz, B. Increase in the stimulation-induced overflow of glutamate by fluoroacetate, a selective inhibitor of the glial tricarboxylic cycle. *Brain Res.* **410**, 116–120 (1987).
35. Rusakov, D. A. & Fine, A. Extracellular Ca^{2+} depletion contributes to fast activity-dependent modulation of synaptic transmission in the brain. *Neuron* **37**, 287–297 (2003).
36. Oertner, T. G., Sabatini, B. L., Nimchinsky, E. A. & Svoboda, K. Facilitation at single synapses probed with optical quantal analysis. *Nature Neurosci.* **5**, 657–664 (2002).
37. Scott, R., Ruiz, A., Henneberger, C., Kullmann, D. M. & Rusakov, D. A. Analog modulation of mossy fiber transmission is uncoupled from changes in presynaptic Ca^{2+}. *J. Neurosci.* **28**, 7765–7773 (2008).